Synchronization, re-entry, and failure of spiral waves in a two-layer discrete excitable system

V. B. Kazantsev, V. I. Nekorkin, and D. V. Artyuhin
Radiophysical Department, Nizhny Novgorod State University, 23 Gagarin Ave., 603600 Nizhny Novgorod, Russia

M. G. Velarde
Instituto Pluridisciplinar, Universidad Complutense, Paseo Juan XXIII, No. 1, Madrid 28 040, Spain
(Received 15 May 2000; published 22 December 2000)

A three-dimensional structure composed of two coupled discrete excitable lattices is considered. Each lattice (layer) is a discrete excitable subsystem and using a *local model* of excitation transfer and failure we have estimated the sufficient conditions for it to exhibit spiral waves. Then we show how interlayer synchronization of all motions is possible. Various effects of spiral wave synchronization, re-entry and failure are also investigated.

DOI: 10.1103/PhysRevE.63.016212 PACS number(s): 05.45.−a

I. INTRODUCTION

Spiral and scroll waves in two-dimensional (2D) and three-dimensional (3D) excitable reaction–diffusion media have been intensively studied in recent years [1–20]. In particular, when studying fibrillation and arrythmicity in the heart, it has been found that the appearance and interaction of spiral-like vortices giving rise to wave turbulence phenomena breaks normal rhythmicity [6–8]. In engineering, 3D multilayer reaction–diffusion lattices have been used for information processing including information compression, image recognition, secure communication, etc. [13–15].

Various types of waves or coherent space-time patterns including rotating spirals, target and scroll waves can be observed in reaction–diffusion lattices [15–23]. A particularly useful model is the FitzHugh–Nagumo reaction–diffusion excitable medium used to mimic the dynamics of excitation in mielinated nerve fibers, neural assemblies, heart tissues, etc. Although being a drastically simplified view of reality, yet it captures key features of the dynamics of the excitable medium (excitation threshold, relaxational pulses or spikes, refractory period, etc.). On the other hand, lattices of coupled local units or cells mimic the anatomy of biological fibers and slices of tissue. The heart tissue, for example, is composed of a number interacting cells suitably distributed in space. The interaction is organized with gap junctions which may be approximated with nearest neighbors (weak) resistive coupling. A simple model taking into account the architecture of such systems may be a reaction–diffusion lattice of excitable cells. At variance with the continuous models ''homogenizing'' or ''averaging'' the system at the characteristic spatial scale of the solutions, the lattice model may take into account ''micro-inhomogeneities'' (of cell size order) of the media which may lead, for example, to the phenomena of wave propagation failure studied in bistable and excitable media [24–26].

In this paper we study spiral wave dynamics in a two-layer lattice system of coupled FitzHugh–Nagumo elements. In Sec. II we describe the model. Then, we investigate the onset and formation of spiral waves in a single layer. Attention is paid to the effects of the discrete inhomogeneous character of the medium. We introduce a *local model* of excitation transfer. Section III is devoted to a study of the effects of interlayer interaction in the synchronization and re-entry of spiral waves. Using the local model we study excitation–re-entry mechanisms and show how terminal wave patterns are affected by the strength of the interlayer coupling. In Sec. IV we allow imperfections in the interlayer coupling restricting it to only local or pin contacts between layers. The Conclusion contains a short discussion of the results found.

II. MODEL

Let us consider the following two-layer excitable lattice system:

$$\begin{aligned}
\dot{u}^1_{j,k} &= f(u^1_{j,k}) - v^1_{j,k} + d(\Delta u^1)_{j,k} + h_{j,k}(u^2_{j,k} - u^1_{j,k}),\\
\dot{v}^1_{j,k} &= \varepsilon u^1_{j,k},\\
\dot{u}^2_{j,k} &= f(u^2_{j,k}) - v^2_{j,k} + d(\Delta u^2)_{j,k} + h_{j,k}(u^1_{j,k} - u^2_{j,k}),\\
\dot{v}^2_{j,k} &= \varepsilon u^2_{j,k},\\
j,k &= 1,2,\ldots,N,
\end{aligned} \tag{1}$$

where superscripts ''1'' and ''2'' denote the variables of the first and the second layer, respectively; $(\Delta w)_{j,k}$ is the discrete Laplace operator $(\Delta w)_{j,k} = w_{j+1,k} + w_{j-1,k} + w_{j,k+1} + w_{j,k-1} - 4w_{j,k}$; the coefficient d accounts for the intralayer coupling; the matrix $h_{j,k}$ characterizes the interlayer interaction. We take $f(w) = w(w-a)(1-w)$ with $0 < a < 1$. The system (1) is considered with Neuman and hence nonflux boundary conditions.

With $d=0$ and $h_{j,k}=0$, Eqs. (1) reduce to a two-dimensional system describing the dynamics of the element, cell or unit,

$$\begin{aligned}
\varepsilon \frac{dz}{d\tau} &= f(z) - w,\\
\frac{dw}{d\tau} &= z.
\end{aligned} \tag{2}$$

 ©2000 The American Physical Society

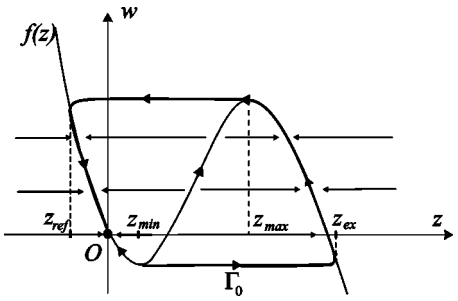

FIG. 1. Phase portrait of the element, cell or unit (2).

For convenience we have rescaled the time, $\tau=\varepsilon t$. With $\varepsilon \to 0$ the dynamics of (2) has both fast and slow features as illustrated in Fig. 1. The system has one stable albeit excitable fixed point O at the origin. This means that for some finite perturbation a trajectory Γ_0 making a long excursion in the phase plane is possible. Along Γ_0 we can define three time intervals corresponding to different (metastable) states of the cell: The *excited* state, S_{ex},

$$S_{\mathrm{ex}}:\{[z(t),w(t)]|z_{\max}<z<z_{\mathrm{ex}}\};$$

the *refractory* state, S_{ref}

$$S_{\mathrm{ref}}:\{[z(t),w(t)]|z_{\mathrm{ref}}<z<0\};$$

and the *rest* state, S_0, when the trajectory evolves in the neighborhood of the fixed point O. Note, that for nonvanishing although small ε, $0<\varepsilon\ll 1$ the slow dynamics does not occur exactly on the curve $f(z)=w$ but in its neighborhood (on slow motion layers whose thickness is of order ε [27]).

With $h_{j,k}=0$ the system (1) splits in two separate layers. Any of these layers, taken separately, represents a discrete excitable medium capable of sustaining spiral waves. Typically to excitable media we obtain spiral wave in a single layer by breaking a plane wave front. The edge of the front starts to twist and after some time takes on a stationary motion. The parameter region, D_{sp}, for spiral wave behavior is shown in Fig. 2. The profile of the spiral wave for the parameters taken far enough from the boundaries is illustrated in Fig. 3(a). The behavior of the tip of the spiral may be rather complex. Depending on parameter values it forms various orbits in the lattice space but we shall not dwell on this issue here.

The boundary of region, D_{sp}, may be split into two parts D_1, D_2. Part D_2 corresponds to the growth of the spiral core as illustrated in Fig. 3(b). When the size of the core is about the lattice size the spiral dies away at its boundary. D_1 is associated with propagation failure caused by the discreteness of the lattice. Upon approaching this boundary the spiral becomes narrower [Fig. 3(c)] and at the end stops propagating.

III. LOCAL MODEL OF EXCITATION TRANSFER AND FAILURE

If the intralayer excitation is strong enough, $d\gg 1$, the discrete system (1) behaves very much like a continuous reaction–diffusion medium. The quasicontinuum approximation of (1) makes sense when the characteristic spatial scale of the solution is much longer than the lattice unit. Waves propagating in such medium do not ''feel'' the local inhomogeneities of the spatial architecture of the lattice. In terms of equations the ODE system (1) can be approximated with a PDE equation with the 2D Laplacian.

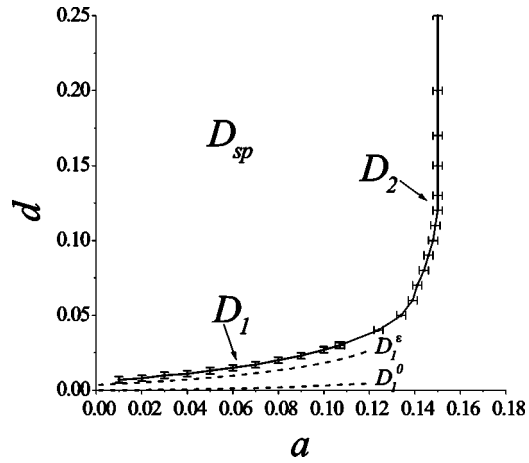

FIG. 2. Region D_{sp} of spiral wave existence in a layer of 100 $\times$100 cells. At the boundary D_2 the spiral wave disappears if it approaches the edges of the layer and at D_1 there is a propagation failure related on the discreteness of the lattice. D_1^0 and D_1^ε are the approximations of D_1 obtained with the ''local model.'' Parameter values: $\varepsilon=0.005$ and $h=0$.

In the opposite case, $d\ll 1$, the solutions are very sensitive to the ''micro-inhomogeneities'' of the lattice. This is the

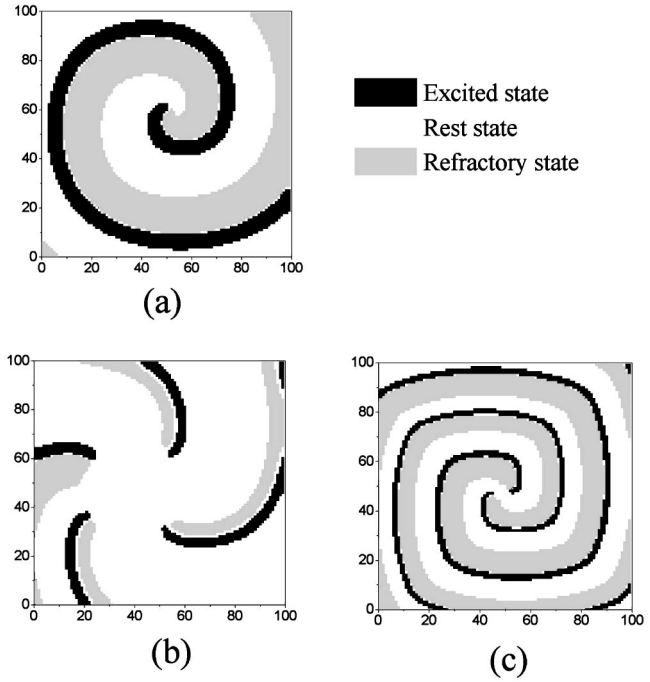

FIG. 3. Snapshots of spiral waves in a layer. (a) Spiral wave for the parameter values ($\varepsilon=0.005, a=0.08, d=0.1$) taken far from the boundaries of D_{sp} (Fig. 2). (b) Spiral wave near the boundary D_2 ($\varepsilon=0.005, a=0.14, d=0.1$) of D_{sp} (Fig. 2). (c) Spiral wave near the boundary D_1 ($\varepsilon=0.005, a=0.08, d=0.022$) of D_{sp} (Fig. 2).

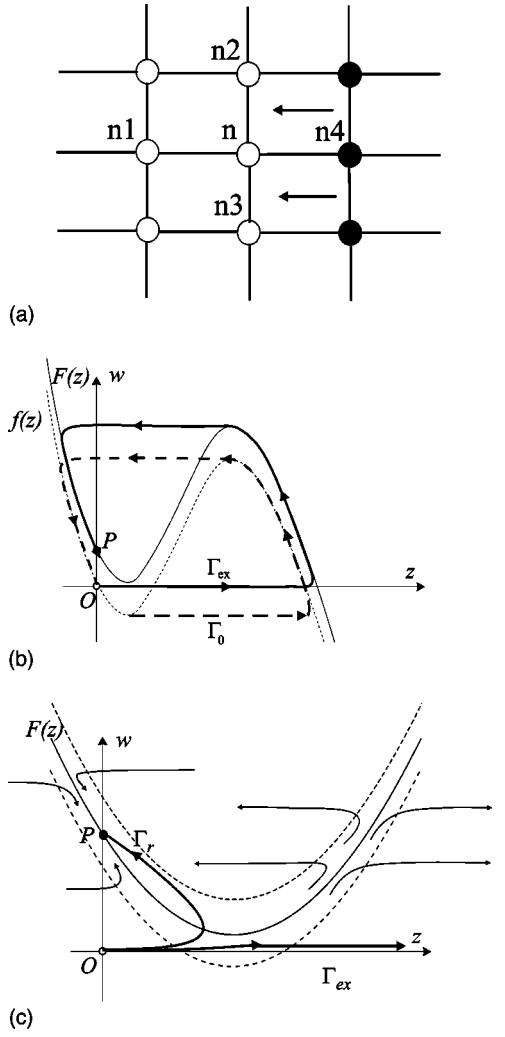

FIG. 4. ''Local model'' of excitation transfer and failure in a layer. (a) Spatial architecture of the layer. Open and solid dots correspond to the rest and excited states of the cells, respectively. Arrows show the direction of excitation transfer. (b) Phase plane representation of the local model. The dashed trajectory, Γ_0, corresponds to the unperturbed cell. Γ_{ex} indicates the excitation of the cell taken from the lattice. (c) Enlarged region of the phase plane near the rest state, *O*, for small nonzero $\varepsilon \ll 1$. Two possibilities of genuine excitation, Γ_{ex}, and its failure.

case we consider here and hence we shall study the dynamics of (1) near the edge of propagation failure (curve D_1 in Fig. 2). As illustrated in Fig. 3(c) the spiral waves in this case become very narrow. They have a squarelike shape composed of a number of interlinked plane-wave fronts. Our aim is to construct, for $d \ll 1$, a drastically reduced albeit significant dynamical system describing the behavior of each local cell of the lattice where the influence of all other cells is adequately parametrized. The basic assumption for designing such a *local model* is the following. As the spiral wave develops the excitation state of the units, S_{ex}, is transmitted *sequentially* from one cell row (column) to another. It is schematically illustrated in Fig. 4(a) where excited and rest cells are shown with solid and open circles, respectively. Let us consider the cell labeled with *n* from the open circle column. From the system (1) we have

$$\varepsilon \dot{z}_n = f(z_n) - w_n + d(z_{n1} + z_{n2} + z_{n3} + z_{n4} - 4z_n),$$
$$\dot{w}_n = z_n . \tag{3}$$

where the z_{ni} $(i=1,2,3,4)$ denote the *u* variables of the four neighboring cells to *n*. When excitation reaches this cell, *n*, we neglect (up to terms of order d^2) the influence of the three unexcited neighbors, $z_{n1}=z_{n2}=z_{n3}=0$. At the same time we take into account the excited cell n_4 with $z_{n4}=z_{ex}$, i.e., with the maximum value of *z* at the excited state (Fig. 1). We take its value from the dynamics of the single cell (2). It is given by the largest root of the equation

$$f(z) - f(z_{\min}) = 0.$$

Thus, we have reduced (1) to the system

$$\varepsilon \dot{z}_n = F(z_n) - w_n ,$$
$$\dot{w}_n = z_n , \tag{4}$$

with $F(z)=f(z)-4\,dz+dz_{ex}$. The function *F* is shifted relative to the unperturbed case, $d=0$, as shown in Fig. 4(b). As the cell is in the rest state the initial conditions for (4) must be taken in the neighborhood of the origin, *O*. Then, the cell *n* will be excited if the trajectory Γ_{ex} exists, i.e., the cell exceeds the excitation threshold.

Let us consider first the case $\varepsilon=0$. Then, the trajectory Γ_{ex} exists if the inequalities

$$F(z^d_{\min}) > 0,$$
$$d < \frac{1-a+a^2}{12}, \tag{5}$$

with

$$z^d_{\min} = \frac{(1+a) - \sqrt{1-a+a^2-12d}}{3}$$

are satisfied. In the parameter space (a,d) the inequalities (5) define the boundary curve D_1^0. As we take the maximum value of the term $d(\Delta z_n)$ in (3) the curve D_1^0 estimates the boundary of the spiral wave propagation failure (Fig. 2). It goes below the curve D_1 obtained by direct numerical integration of Eqs. (1).

Let us now consider a small but nonzero $\varepsilon \ll 1$. As earlier mentioned, now the slow motions occur in thin slow-motion layers near the curve $F(z)=w$. Qualitatively the behavior of system (4) is illustrated in Fig. 4(c). Depending on the parameter values there are various routes of the trajectory originated at point *O*. The two trajectories Γ_r and Γ_{ex} shown correspond to the failure of excitation and its transfer, respectively. Thus, if the trajectory Γ exists in system (4),

$$\Gamma : \{[z(t), w(t)] \,|\, z(0)=w(0)=0, \quad z(t) < z_{\max}, \quad \forall t > 0\} \tag{6}$$

the excitation fails to propagate. The boundary curve, D_1^e obtained with the condition (6) is shown in Fig. 2. A rather good qualitative and quantitative agreement with the experimental curve D_1 can be observed.

Note, that as we take the maximum value, z_{ex}, at the excited state, S_{ex}, of the cell what we find are *sufficient* conditions for the propagation failure. For the parameters taken in the neighborhood above the boundary D_1^e the cell is ''less excited,'' $z_{\max} \leqslant z < z_{ex}$ and the wave may fail at the next grid of the lattice.

IV. SPIRAL WAVES IN THE TWO-LAYER LATTICE SYSTEM

Let us first consider the system (1) with uniform interlayer coupling, and hence all $h_{j,k}=h\neq 0$.

A. Global interlayer synchronization

By changing variables

$$x_{j,k}=u_{j,k}^1-u_{j,k}^2 \quad y_{j,k}=v_{j,k}^1-v_{j,k}^2,$$

$$x_{j,k}^+=u_{j,k}^1+u_{j,k}^2 \quad y_{j,k}^+=v_{j,k}^1+v_{j,k}^2,$$

the system (1) becomes

$$\begin{aligned}
\dot{x}_{j,k}&=G(x_{j,k},x_{j,k}^+)-y_{j,k}+d(\Delta x)_{j,k}-2hx_{j,k},\\
\dot{y}_{j,k}&=\varepsilon x_{j,k},\\
\dot{x}_{j,k}^+&=G^+(x_{j,k},x_{j,k}^+)-y_{j,k}^++d(\Delta x^+)_{j,k},\\
\dot{y}_{j,k}^+&=\varepsilon x_{j,k}^+,
\end{aligned} \tag{7}$$

with

$$j,k=1,2,\ldots,N,$$

$$G(x_{j,k},x_{j,k}^+)=f(u_{j,k}^1)-f(u_{j,k}^2),$$

$$G^+(x_{j,k},x_{j,k}^+)=f(u_{j,k}^1)+f(u_{j,k}^2),$$

For (7), $M=\{x_{j,k}=y_{j,k}=0\}$ is the manifold of synchronous motions or the interlayer synchronization manifold. Let us show that M is globally asymptotically stable. Consider the function

$$V=\sum_{j,k=1}^{N}\frac{x_{j,k}^2}{2}+\frac{y_{j,k}^2}{2\varepsilon}.$$

Its derivative along the flow (7) is

$$\dot{V}=-\sum_{j,k=1}^{N}(P_{j,k}+Q_{j,k})$$

with

$$\begin{aligned}
P_{j,k}=&-d(x_{j,k}x_{j-1,k}+x_{j,k}x_{j,k-1})+px_{j,k}^2\\
&-d(x_{j,k}x_{j+1,k}+x_{j,k}x_{j,k+1}),
\end{aligned}$$

$$Q_{j,k}=x_{j,k}^2\left[\frac{1}{4}(x_{j,k}^2+3y_{j,k}^2)-(1+a)y_{j,k}+\frac{(1+a)^2}{3}\right],$$

and

$$p=4d+2h-\frac{1-a+a^2}{3}.$$

Then all $Q_{j,k}$ are positive definite and, consequently, the quantity $P=\sum_{j,k=1}^{N}P_{j,k}$ is also positive definite. Indeed, consider the vector $r=(r_1,r_2,\ldots,r_{N^2})$, where $r_1=x_{11}, r_2=x_{12},\ldots,r_{N^2}=x_{NN}$. Using these coordinates the function P becomes the quadratic form

$$P=\sum_{i,j=1}^{N^2}a_{i,j}r_ir_j=r^TAr,$$

with $a_{ij}=a_{ji}$, the superscript T denotes the transpose and $A=||a_{i,j}||$ is a square symmetric $N^2\times N^2$ matrix. The quadratic form P will be positive definite if the eigenvalues of the symmetric matrix A are positive [28]. Applying Gershgorin theorem to the matrix A we find that if $p>4d$ then the union of the Gershgorin disks corresponding to the matrix A is located to the right of the imaginary axis [29]. Thus, the inequality

$$h>h^*=\frac{1-a+a^2}{6} \tag{8}$$

ensures the positiveness of all eigenvalues of the matrix A and, consequently, the form P is positive definite when condition (8) is satisfied. Therefore, $\dot{V}<0$ holds outside the manifold M and $\dot{V}=0$ on the manifold, and hence V is a Lyapunov potential function. Thus, the synchronization manifold M is globally asymptotically stable. Accordingly, whatever the initial conditions, all motions in the system (1) synchronize if the parameters satisfy (8).

B. Interlayer reentry and synchronization

Let the initial conditions for (1) be a spiral wave in the first layer and the rest state in the other. When (8) is satisfied and the interlayer coupling, h, is strong enough the layers synchronize and each of them exhibits a spiral wave identical to the initial one. Note that the threshold of excitation, accounted in the model by parameter a, is very low (Fig. 2) and the cells of the second layer are easily excited and enslaved by the pattern existing in the first layer. This corresponds to a rather rigid interlayer interaction.

For values of h lower than those of region (8) the interaction becomes more ''elastic'' and due to the bi-directional interlayer coupling various re-entry phenomena are possible.

In the parameter plane (h,d), for fixed $a=0.01$, four salient regions exist where the interlayer dynamics is drastically different (Fig. 5).

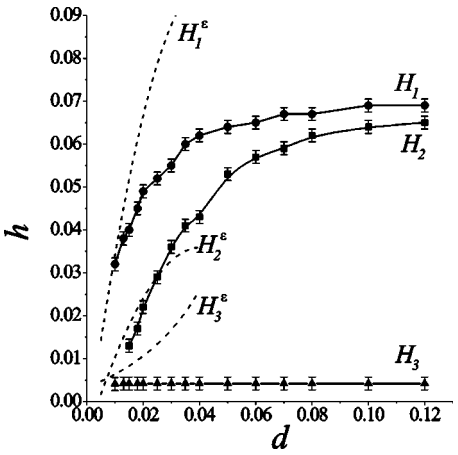

FIG. 5. Boundaries H_1, H_2, H_3 of various outcome of the interlayer interaction obtained by numerical simulation of Eqs. (1). $H_1^\varepsilon, H_2^\varepsilon, H_3^\varepsilon$ have been obtained with the ''local model.'' Parameter values: $\varepsilon = 0.005$ and $a = 0.01$.

(i) In the region above the curve H_1 the terminal (synchronized) patterns represent identical spiral waves with cores slightly shifted in the lattice space (Fig. 6). Thus, the spiral wave dominates the rest state preserving all its key features (shape, period, and amplitude). The perturbation of the spiral core shown in the sequence of snapshots in Fig. 6 is associated with the lower oscillation amplitude of the cells at the tip of the spiral. Here the influence of the second layer (feedback) is stronger relative to all other cells and it is sufficient to perturb the excited state in the first layer.

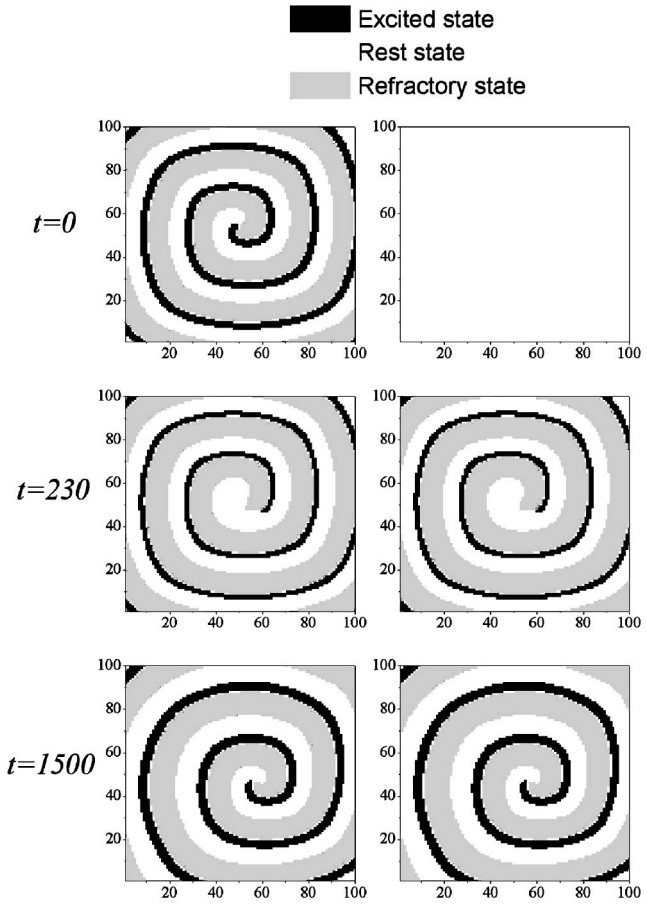

FIG. 6. Sequence of snapshots illustrating spiral wave synchronization in the region above the curve H_1 (Fig. 5). Parameter values: $\varepsilon = 0.005$, $a = 0.01$, $d = 0.01$, and $h = 0.06$.

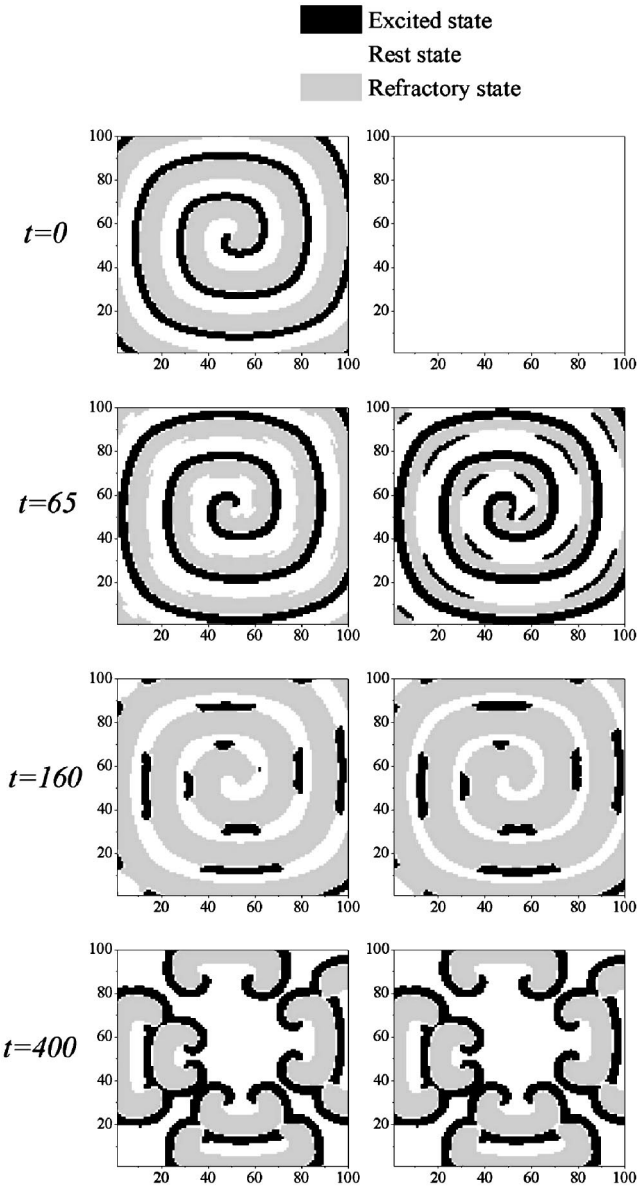

FIG. 7. Sequence of snapshots illustrating spiral wave re-entry leading to the breakdown of the original stimulus in the region between the curves H_1 and H_2 (Fig. 5). Parameter values: $\varepsilon = 0.005$, $a = 0.01$, $d = 0.01$, and $h = 0.045$.

(ii) In the region between the curves H_1 and H_2 (Fig. 5), as a result of the sequence of interlayer re-entries, two offspring wave patterns appear evolving in rather complex way (Fig. 7). This complexity comes from the cooperative influence of intralayer collisions and interlayer excitation and inhibition. As earlier said, for the case of very low intralayer coupling one must take into account the microinhomogeneities of the lattice architecture. As we consider squarelike connections [Fig. 4(a)], or four nearest-neighbor

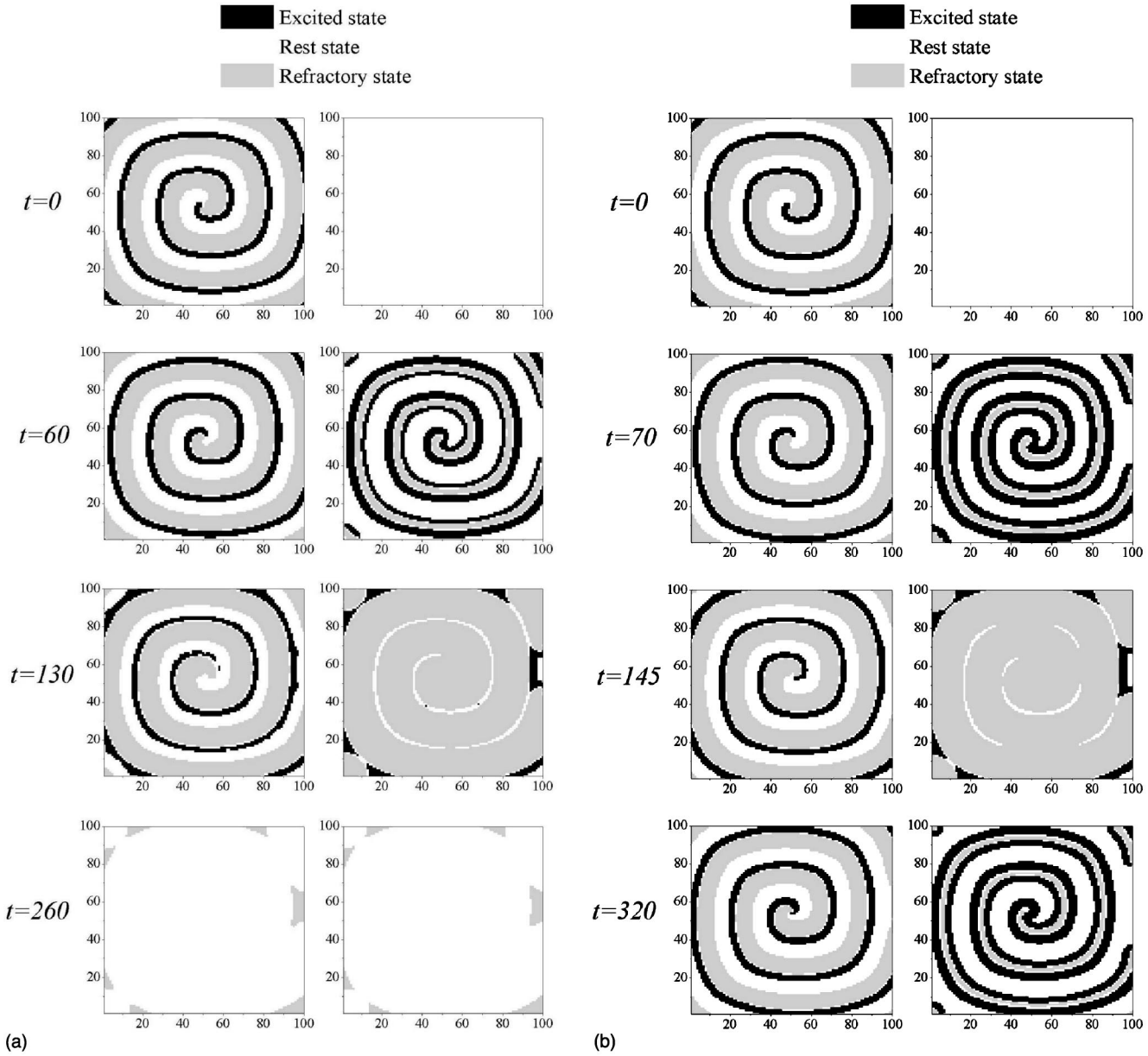

FIG. 8. (a) Sequence of snapshots illustrating spiral wave re-entry leading to the disappearance of the original stimulus in the region between the curves H_2 and H_3 (Fig. 5). Parameter values: $\varepsilon=0.005$, $a=0.01$, $d=0.01$, and $h=0.03$. (b) Corresponding sequence of snapshots illustrating cyclic spiral wave re-entry in the region near the curve H_3. Parameter values: $\varepsilon=0.005$, $a=0.01$, $d=0.01$, and $h=0.01$.

coupling, the wave properties are anisotropic and hence a squarelike rough shape of the spiral waves appears [Fig. 3(c)]. Figure 7 illustrates that, as time proceeds, in the second lattice a number of fronts appear and travel in the diagonal direction. Then, the fronts collide with the spiral and disappear. The cells of the second layer come to the refractory state and this inhibits their companion cells in the first layer. As the result of such feedforward-feedback influence two identical patterns appear and evolve synchronously in the two-layer lattice system.

(iii) Further lowering the interlayer coupling strength, h, brings us to the region located between the curves H_2 and H_3 (Fig. 5) where the spiral wave stimulus can disappear as a consequence of inter-layer reentry [Fig. 8(a)]. At first, the spiral wave perturbs the motionless elements of the second layer and forms a spiral wave shape excitation. Subsequently, this excitation yields two spiral waves traveling in opposite directions. Then the two waves collide and disappear. Then almost all elements of the second layer come to their refractory states. Consequently, the feedback inhibits all motions in the first layer and both layers come to the rest state. However, for some parameter values (close to the curve H_3) the feedback is not strong enough to inhibit motions in the first layer and the original spiral is preserved as shown in Fig. 8(b). We have a *re-entry cycle* operating with approximately the period of the spiral wave.

(iv) Too low interlayer coupling in the region below H_3 (Fig. 5) does not permit excitation in the second layer. Here

the spiral wave is preserved evolving with slightly different shape and period.

Note that for high enough values of d the lattice behavior approaches that of the continuous medium. As mentioned in Sec. II the shape of the spiral becomes smoother [Figs. 3(a) and 3(b)] and hence there is negligible spatial anisotropy. Then, the region (ii) becomes smaller and disappears with $d \gg 1$. Such tendency can be seen in Fig. 5 where the curves H_1 and H_2 approach each other. Further increase of d makes the ''size'' of the spiral about the size of the layers and the outcome of the interlayer interaction becomes very sensitive to the boundary conditions. We do not consider their influence here.

C. Local model of the interlayer reentry

Let us assume that both the intralayer and the interlayer coupling are very weak, $h \ll 1$ and $d \ll 1$. Then, as done for a single layer we can qualitatively divide the evolution of system (1) into a sequence of excitation transfer events from cell to cell. Let us apply the local model approach (3),(4),(5),(6) with both intralayer and interlayer interactions taken into account.

(i) Let us first estimate the conditions for interlayer excitation failure, i.e. the boundary H_3 (Fig. 5). A schematic representation is shown in Fig. 9(a). Consider that a plane wave front of excitation is propagating in the first layer while all the cells of the second one are at rest. When the interlayer interaction is switched-on we can approximately describe the dynamics of the cell n taken from the second layer by the system (4) with the nonlinear function

$$F(z) = f(z) - (4d + h)z + hz_{\mathrm{ex}}. \tag{9}$$

Then, for $\varepsilon \to 0$ there is excitation failure when

$$F(z^h_{\min}) < 0, \qquad (h + 4d) < \frac{1 - a + a^2}{3}, \tag{10}$$

with

$$z^h_{\min} = \frac{(1+a) - \sqrt{1 - a + a^2 - 12d - 3h}}{3}.$$

The inequalities (10) define the region below the boundary curve H_3^0 in the parameter plane (h,d) (Fig. 10). For $\varepsilon \ll 1$, but nonzero, taking into account the dynamics in the slow motion layers [Fig. 4(c)] we obtain for (4) with (9) the condition (6). The boundary curve H_3^ε is shown in Fig. 10.

Let the values of h be high enough to excite the second layer.

(ii) When the stimulus is a plane wave front traveling in the longitudinal direction, an excitation of identical shape in the second layer splits into two parts, one proceeding forward synchronously with the original front and another moving backward [Figs. 7 and 9(b)]. As the backward moving front reaches the cells inhibited by the refractory ones of the first layer, it may fail to propagate. For the cell n in Fig. 9(b) we have system (4) with

$$F(z) = f(z) - (4d + h)z + dz_{\mathrm{ex}} + hz_{\mathrm{ref}}, \tag{11}$$

where z_{ref} denotes the refractory state of the cell. We take its value from the dynamics of a single cell (2) (Fig. 1). It is given by the lowest root of the equation

$$f(z) - f(z_{\max}) = 0.$$

Then, the boundaries of the region for the backward traveling front to be inhibited are defined by (10) with (11) for $\varepsilon = 0$, and by (4) and (6) with (11) for $\varepsilon \ll 1$, respectively. These inequalities are satisfied above the curves H_2^0 and H_2^ε

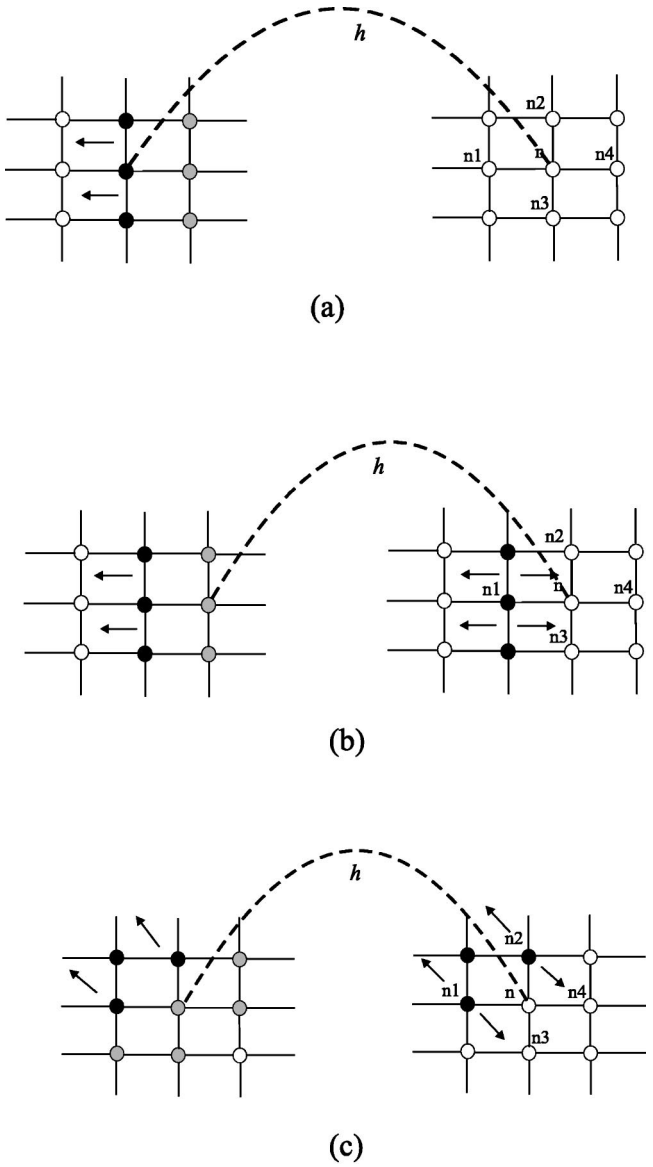

FIG. 9. Schematic representation of excitation re-entry in interacting two-layer lattice system. (a) Entry of excitation to layer at rest. (b) Inhibition of excitation along the longitudinal direction. (c) Inhibition of excitation along the diagonal direction.

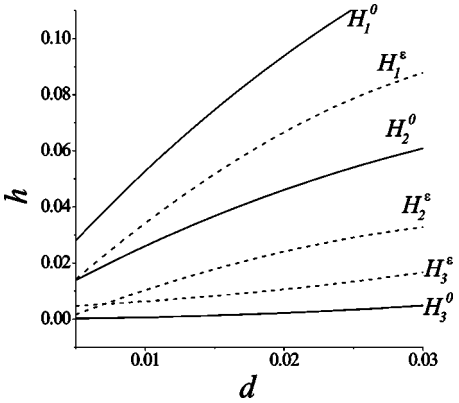

FIG. 10. ''Local model'' prediction for the excitation inhibition in the parameter plane (h,d) for $\varepsilon=0$, H_1^0,H_2^0,H_3^0 (solid lines), and for $\varepsilon=0.005$, $H_1^\varepsilon,H_2^\varepsilon,H_3^\varepsilon$ (broken lines).

shown in Fig. 10. At variance with the case of local excitation failure in a single layer the cell at rest n [Fig. 9(b)] tends to be excited by the neighboring cells of its own layer (with the ''strength'' accounted by d) and to be inhibited by the corresponding refractory cell from the first layer (accounted by h). Hence, the curve H_2 gives a critical h/d ratio above which only a forward traveling (synchronized) front appears in the second lattice.

(iii) Let us consider the wave front propagating in a diagonal direction. As in case (ii) we have for the cell n [Fig. 9(c)] system (4) with

$$F(z)=f(z)-(4d+h)z+2dz_{\mathrm{ex}}+hz_{\mathrm{ref}}. \qquad (12)$$

Then, the regions of excitation failure in the diagonal direction are defined by (10) with (12) for $\varepsilon=0$ (above the curve H_1^0) and by (4) and (6) with (12) for $\varepsilon\ll 1$ (above the curve H_1^ε), respectively.

As in the previous case the curve H_1 provides the relation between the interlayer and intralayer coupling above which only a synchronized front is possible in the diagonal direction. The spiral wave for small d [Fig. 3(c)] may be qualitatively divided into a number of plane fronts traveling in the longitudinal (horizontal or vertical) direction ''interconnected'' with ''portions'' propagating in the diagonal direction. Hence, above the curve H_1 there is synchronization in both directions and we end up with synchronized spirals (Fig. 6). Between the curves H_1 and H_2 the ''diagonal'' synchronization fails and there is a sequence of re-entries breaking the original spiral (Fig. 7). Below H_2 we obtain the backward traveling spiral wave of continuous shape (Fig. 8).

To compare the results predicted with the local model with data obtained with the numerical integration of Eqs. (1) we put them together in Fig. 5. The curves H_i^ε give a very good approximation of the boundaries H_i for low enough values of d and h. Note, that the curves H_2^ε and H_1^ε intersect when $d=d_2^*$. Thus, for $d<d_2^*$ for all values of h taken above the curve H_3^ε the original spiral wave cannot be completely destroyed in the collision of the two secondary spirals with opposite ''charges'' [Figs. 8(a) and 8(b)]. This phenomenon is verified numerically as the curve H_2 ends up with

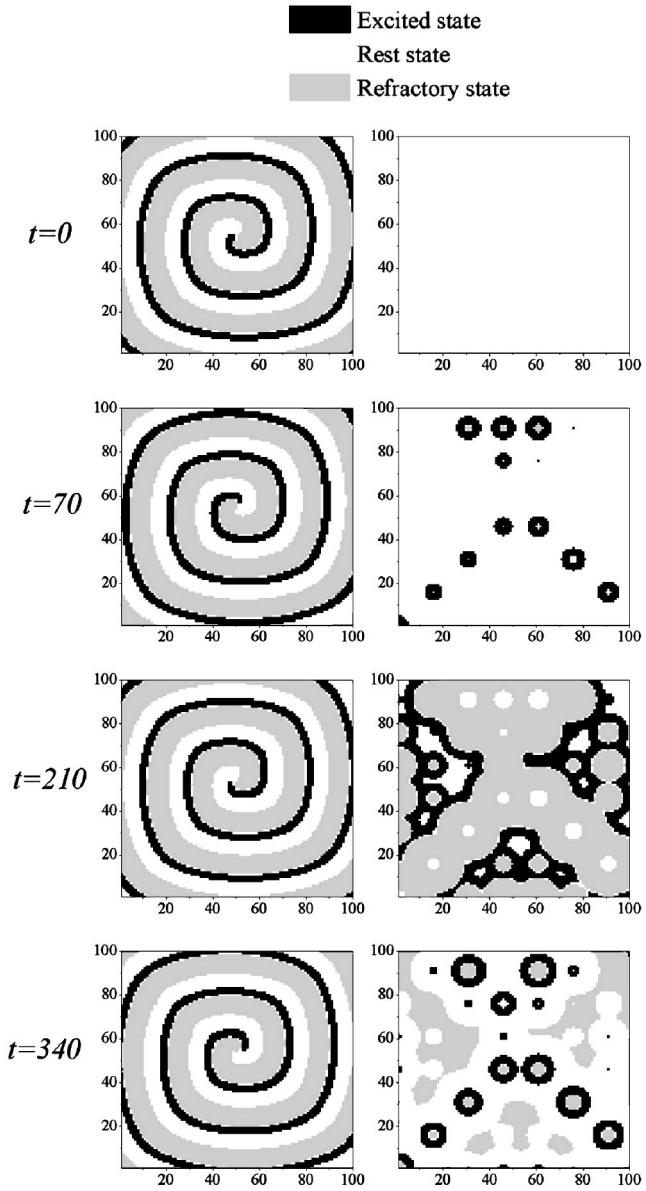

FIG. 11. Sequence of snapshots illustrating the outcome of ill-functioning interlayer synchronization obtained with coupling matrix $h_{j,k}$ with $\Delta=15$. Parameter values: $\varepsilon=0.005$, $a=0.01$, $d=0.03$, and $h=0.06$.

$d\approx 0.015$. For lower values of d the outcome of the system is wave patterns like those shown in Fig. 7.

V. RAREFIED INTERLAYER CONNECTIONS

In problems where lattice dynamics may have an application like in the study of heart fibrillation and failure there are always domains, sites or bonds, which are ill-functioning or broken. Dynamically, such domains are not capable to provide a proper transfer of excitation in the tissue. Let us now study how such rarefied coupling affects the synchronization and wave pattern replication processes when some bonds $h_{j,k}$ are ill-functioning or broken.

Let now $h_{j,k}$ be defined in the matrix form

$$h_{j,k}=\sum_{j',k'}^{N} h\,\delta_{\Delta j',j}\delta_{\Delta k',k},$$

$$j,k=1,2,\ldots,N,$$

where $\Delta=1,2,3,\ldots$ denotes the spatial coupling grid and δ is Kroneker symbol. When Δ is much smaller than a characteristic space scale of the initial spiral wave, which depends on *d*, the interlayer interaction occurs as with a homogeneous coupling. The increase of Δ leads to the destruction of the initial spiral wave even for high values of *h*. Along the well-functioning sites the excitation is transferred to the layer at rest where it may yield a sequence of target waves (Fig. 11). Then, those target waves interfere in some complex way creating a new wave pattern. As shown in Fig. 11 collisions may create large areas or clusters of cells in the refractory state. At variance with the homogeneous case [Fig. 7(a)] the feedback from such cells cannot inhibit the original spiral wave in the first layer. The feedback is transferred through a scarce number of well-functioning sites and hence only locally the spiral wave is perturbed. Subsequently, the wave recovers its form. Note, that when, for example, there is a large cluster of well-functioning sites, the feedback may destroy the original spiral. We do not consider this case here.

VI. CONCLUSION

We have studied salient features of the dynamics of a two-layer discrete FitzHugh–Nagumo reaction–diffusion architecture. After finding, for a single layer, the region of existence of spiral waves, we have analytically predicted and numerically obtained the boundary of wave propagation failure originated in the discreteness of the medium. Then for the system composed of two interacting such layers we have investigated the processes of spiral wave synchronization, re-entry and failure. We have identified some re-entry loops of excitation transfer from layer to layer resulting in the disappearance of the spiral wave or its breaking into a seemingly complex wave pattern. The interlayer interaction allows a spiral wave stimulus to be replicated in another layer at rest, or yields a complex wave pattern breaking the original (''normal'') rhythmicity of the system, or it can be completely destroyed bringing all cells to the rest state. As expected, the spiral-wave dynamics in a two-layer lattice system drastically depends on the micro-inhomogeneities of the discrete lattice architecture and its anisotropy.

ACKNOWLEDGMENTS

This research has been supported by the BBV Foundation, by the Russian Foundation for Basic Research under Grant No. 00-02-16400 (Russia), and by DGICYT (Spain) under Grant No. PB96-0599.

[1] J. D. Murray, *Mathematical Biology*, 2nd ed. (Springer-Verlag, Berlin, 1993).
[2] A. T. Winfree, *The Geometry of Biological Time*, 2nd ed. (Springer-Verlag, Berlin, 1990).
[3] A. M. Zhabotinsky, *Concentration Auto-oscillations* (Nauka, Moscow, 1974) (in Russian).
[4] V. A. Davidov and A. S. Mihailov, *Nonlinear Waves, Structures and Bifurcations* (Nauka, Moscow, 1987) (in Russian).
[5] V. S. Zykov, *Modelling of Wave Processes in Excitable Media* (Manchester University Press, Manchester, 1988).
[6] V. I. Krinsky, A. B. Medvedinsky, and A. V. Panfilov, *Mathematical Cybernetics* **8**, 1 (1986) (in Russian).
[7] V. N. Biktashev, A. V. Holden, S. F. Mironov, A. M. Pertsov, and A. V. Zaitsev, Int. J. Bifurcation Chaos Appl. Sci. Eng. **9**, 695 (1999).
[8] V. N. Biktashev, Int. J. Bifurcation Chaos Appl. Sci. Eng. **8**, 677 (1998).
[9] A. V. Panfilov and A. V. Holden, Phys. Lett. A **147**, 463 (1990).
[10] T. Ohta, Y. Hayase, and R. Kobayashi, Phys. Rev. E **54**, 6074 (1996).
[11] T. Erneux and G. Nicolis, Physica D **67**, 237 (1993).
[12] A. Babloyantz and C. Lourenco, Proc. Natl. Acad. Sci. U.S.A. **91**, 9027 (1994).
[13] P. Thiran, *Dynamics and Self-organization of Locally Coupled Neural Networks* (Presses Polytechniques et Universitaires Romandes, Lausanne, 1997).
[14] R. Linsker, Annu. Rev. Neurosci. **13**, 257 (1990).
[15] G. Manganaro, P. Arena, and L. Fortuna, *Cellular Neural Newtworks. Chaos, Complexity and VLSI Processing* (Springer-Verlag, Berlin, 1999).
[16] L. Pivka, IEEE Trans. Circuits Syst. **42**, 638 (1995).
[17] M. J. Ogorzalek, Z. Galias, A. M. Dabrowski, and W. R. Dabrowski, IEEE Trans. Circuits Syst. **42**, 706 (1995).
[18] M. G. Velarde, V. I. Nekorkin, V. B. Kazantsev, and J. Ross, Proc. Natl. Acad. Sci. U.S.A. **94**, 5024 (1997).
[19] V. I. Nekorkin, V. B. Kazantsev, M. I. Rabinovich, and M. G. Velarde, Phys. Rev. E **57**, 3344 (1998).
[20] V. I. Nekorkin, V. B. Kazantsev, and M. G. Velarde, Phys. Rev. E **58**, 1764 (1998).
[21] C. Elphick, A. Hagberg, and E. Meron, Phys. Rev. E **51**, 3052 (1998).
[22] A. Hagberg and E. Meron, Phys. Rev. E **57**, 299 (1998).
[23] A. F. M. Maŕee and A. V. Panfilov, Phys. Rev. E **78**, 1819 (1997).
[24] V. I. Nekorkin, V. A. Makarov, V. B. Kazantsev, and M. G. Velarde, Physica D **100**, 330 (1997).
[25] J. P. Keener, SIAM (Soc. Ind. Appl. Math.) J. Appl. Math. **47**, 556 (1987).
[26] J. P. Keener, Physica D **136**, 1 (2000).
[27] *The Modern Problems of Mathematics. Fundamental Directions*, edited by V. I. Arnold (VINITI, Moscow, 1986) (in Russian), Vol. 5.
[28] R. N. V. Tu, *Dynamic Systems. An Introduction with Applications in Economics and Biology* (Springer-Verlag, Berlin, 1994).
[29] R. Horn and V. Johnson, *Matrix Analysis* (Cambridge University Press, Cambridge, 1986), Chap. 7.